Search for a Narrow Baryonic Resonance
Decaying to $K_s^0 p$ or $K_s^0 \bar{p}$
in Deep Inelastic Scattering at HERA

H1 Collaboration

Abstract

A search for a narrow baryonic resonance decaying to $K_s^0 p$ or $K_s^0 \bar{p}$ is carried out in deep inelastic ep scattering with the H1 detector at HERA. Such a resonance could be a strange pentaquark Θ^+, evidence for which has been reported by several experiments. The $K_s^0 p$ and $K_s^0 \bar{p}$ invariant mass distributions presented here do not show any significant peak in the mass range from threshold up to 1.7 GeV. Mass dependent upper limits on $\sigma(ep \rightarrow e\Theta^+ X) \times BR(\Theta^+ \rightarrow K^0 p)$ are obtained at the 95% confidence level.

A. Aktas[9], V. Andreev[25], T. Anthonis[3], B. Antunovic[26], S. Aplin[9], A. Asmone[33],
A. Astvatsatourov[3], A. Babaev[24,†], S. Backovic[30], A. Baghdasaryan[37], P. Baranov[25],
E. Barrelet[29], W. Bartel[9], S. Baudrand[27], S. Baumgartner[39], J. Becker[40], M. Beckingham[9],
O. Behnke[12], O. Behrendt[6], A. Belousov[25], N. Berger[39], J.C. Bizot[27], M.-O. Boenig[6],
V. Boudry[28], J. Bracinik[26], G. Brandt[12], V. Brisson[27], D. Bruncko[15], F.W. Büsser[10],
A. Bunyatyan[11,37], G. Buschhorn[26], L. Bystritskaya[24], A.J. Campbell[9], F. Cassol-Brunner[21],
K. Cerny[32], V. Cerny[15,46], V. Chekelian[26], J.G. Contreras[22], J.A. Coughlan[4], B.E. Cox[20],
G. Cozzika[8], J. Cvach[31], J.B. Dainton[17], W.D. Dau[14], K. Daum[36,42], Y. de Boer[24],
B. Delcourt[27], M. Del Degan[39], A. De Roeck[9,44], E.A. De Wolf[3], C. Diaconu[21], V. Dodonov[11],
A. Dubak[30,45], G. Eckerlin[9], V. Efremenko[24], S. Egli[35], R. Eichler[35], F. Eisele[12], A. Eliseev[25],
E. Elsen[9], S. Essenov[24], A. Falkewicz[5], P.J.W. Faulkner[2], L. Favart[3], A. Fedotov[24], R. Felst[9],
J. Feltesse[8], J. Ferencei[15], L. Finke[10], M. Fleischer[9], G. Flucke[33], A. Fomenko[25], G. Franke[9],
T. Frisson[28], E. Gabathuler[17], E. Garutti[9], J. Gayler[9], C. Gerlich[12], S. Ghazaryan[37],
S. Ginzburgskaya[24], A. Glazov[9], I. Glushkov[38], L. Goerlich[5], M. Goettlich[9], N. Gogitidze[25],
S. Gorbounov[38], C. Grab[39], T. Greenshaw[17], M. Gregori[18], B.R. Grell[9], G. Grindhammer[26],
C. Gwilliam[20], D. Haidt[9], L. Hajduk[5], M. Hansson[19], G. Heinzelmann[10],
R.C.W. Henderson[16], H. Henschel[38], G. Herrera[23], M. Hildebrandt[35], K.H. Hiller[38],
D. Hoffmann[21], R. Horisberger[35], A. Hovhannisyan[37], T. Hreus[3,43], S. Hussain[18],
M. Ibbotson[20], M. Ismail[20], M. Jacquet[27], L. Janauschek[26], X. Janssen[3], V. Jemanov[10],
L. Jönsson[19], D.P. Johnson[3], A.W. Jung[13], H. Jung[19,9], M. Kapichine[7], J. Katzy[9],
I.R. Kenyon[2], C. Kiesling[26], M. Klein[38], C. Kleinwort[9], T. Klimkovich[9], T. Kluge[9], G. Knies[9],
A. Knutsson[19], V. Korbel[9], P. Kostka[38], K. Krastev[9], J. Kretzschmar[38], A. Kropivnitskaya[24],
K. Krüger[13], M.P.J. Landon[18], W. Lange[38], G. Laštovička-Medin[30], P. Laycock[17],
A. Lebedev[25], G. Leibenguth[39], V. Lendermann[13], S. Levonian[9], L. Lindfeld[40], K. Lipka[38],
A. Liptaj[26], B. List[39], J. List[10], E. Lobodzinska[38,5], N. Loktionova[25], R. Lopez-Fernandez[23],
V. Lubimov[24], A.-I. Lucaci-Timoce[9], H. Lueders[10], D. Lüke[6,9], T. Lux[10], L. Lytkin[11],
A. Makankine[7], N. Malden[20], E. Malinovski[25], S. Mangano[39], P. Marage[3], R. Marshall[20],
L. Marti[9], M. Martisikova[9], H.-U. Martyn[1], S.J. Maxfield[17], A. Mehta[17], K. Meier[13],
A.B. Meyer[9], H. Meyer[36], J. Meyer[9], V. Michels[9], S. Mikocki[5], I. Milcewicz-Mika[5],
D. Milstead[17], D. Mladenov[34], A. Mohamed[17], F. Moreau[28], A. Morozov[7], J.V. Morris[4],
M.U. Mozer[12], K. Müller[40], P. Murín[15,43], K. Nankov[34], B. Naroska[10], Th. Naumann[38],
P.R. Newman[2], C. Niebuhr[9], A. Nikiforov[26], G. Nowak[5], K. Nowak[40], M. Nozicka[32],
R. Oganezov[37], B. Olivier[26], J.E. Olsson[9], S. Osman[19], D. Ozerov[24], V. Palichik[7],
I. Panagoulias[9], T. Papadopoulou[9], C. Pascaud[27], G.D. Patel[17], H. Peng[9], E. Perez[8],
D. Perez-Astudillo[22], A. Perieanu[9], A. Petrukhin[24], D. Pitzl[9], R. Plačakytė[26], B. Portheault[27],
B. Povh[11], P. Prideaux[17], A.J. Rahmat[17], N. Raicevic[30], P. Reimer[31], A. Rimmer[17], C. Risler[9],
E. Rizvi[18], P. Robmann[40], B. Roland[3], R. Roosen[3], A. Rostovtsev[24], Z. Rurikova[26],
S. Rusakov[25], F. Salvaire[10], D.P.C. Sankey[4], E. Sauvan[21], S. Schätzel[9], S. Schmidt[9],
S. Schmitt[9], C. Schmitz[40], L. Schoeffel[8], A. Schöning[39], H.-C. Schultz-Coulon[13], F. Sefkow[9],
R.N. Shaw-West[2], I. Sheviakov[25], L.N. Shtarkov[25], T. Sloan[16], P. Smirnov[25], Y. Soloviev[25],
D. South[9], V. Spaskov[7], A. Specka[28], M. Steder[9], B. Stella[33], J. Stiewe[13], A. Stoilov[34],
U. Straumann[40], D. Sunar[3], V. Tchoulakov[7], G. Thompson[18], P.D. Thompson[2], T. Toll[9],
F. Tomasz[15], D. Traynor[18], P. Truöl[40], I. Tsakov[34], G. Tsipolitis[9,41], I. Tsurin[9], J. Turnau[5],
E. Tzamariudaki[26], K. Urban[13], M. Urban[40], A. Usik[25], D. Utkin[24], A. Valkárová[32],
C. Vallée[21], P. Van Mechelen[3], A. Vargas Trevino[6], Y. Vazdik[25], C. Veelken[17], S. Vinokurova[9],
V. Volchinski[37], K. Wacker[6], G. Weber[10], R. Weber[39], D. Wegener[6], C. Werner[12],

M. Wessels[9], B. Wessling[9], Ch. Wissing[6], R. Wolf[12], E. Wünsch[9], S. Xella[40], W. Yan[9], V. Yeganov[37], J. Žáček[32], J. Zálešák[31], Z. Zhang[27], A. Zhelezov[24], A. Zhokin[24], Y.C. Zhu[9], J. Zimmermann[26], T. Zimmermann[39], H. Zohrabyan[37], and F. Zomer[27]

[1] *I. Physikalisches Institut der RWTH, Aachen, Germany[a]*
[2] *School of Physics and Astronomy, University of Birmingham, Birmingham, UK[b]*
[3] *Inter-University Institute for High Energies ULB-VUB, Brussels; Universiteit Antwerpen, Antwerpen; Belgium[c]*
[4] *Rutherford Appleton Laboratory, Chilton, Didcot, UK[b]*
[5] *Institute for Nuclear Physics, Cracow, Poland[d]*
[6] *Institut für Physik, Universität Dortmund, Dortmund, Germany[a]*
[7] *Joint Institute for Nuclear Research, Dubna, Russia*
[8] *CEA, DSM/DAPNIA, CE-Saclay, Gif-sur-Yvette, France*
[9] *DESY, Hamburg, Germany*
[10] *Institut für Experimentalphysik, Universität Hamburg, Hamburg, Germany[a]*
[11] *Max-Planck-Institut für Kernphysik, Heidelberg, Germany*
[12] *Physikalisches Institut, Universität Heidelberg, Heidelberg, Germany[a]*
[13] *Kirchhoff-Institut für Physik, Universität Heidelberg, Heidelberg, Germany[a]*
[14] *Institut für Experimentelle und Angewandte Physik, Universität Kiel, Kiel, Germany*
[15] *Institute of Experimental Physics, Slovak Academy of Sciences, Košice, Slovak Republic[f]*
[16] *Department of Physics, University of Lancaster, Lancaster, UK[b]*
[17] *Department of Physics, University of Liverpool, Liverpool, UK[b]*
[18] *Queen Mary and Westfield College, London, UK[b]*
[19] *Physics Department, University of Lund, Lund, Sweden[g]*
[20] *Physics Department, University of Manchester, Manchester, UK[b]*
[21] *CPPM, CNRS/IN2P3 - Univ. Mediterranee, Marseille - France*
[22] *Departamento de Fisica Aplicada, CINVESTAV, Mérida, Yucatán, México[j]*
[23] *Departamento de Fisica, CINVESTAV, México[j]*
[24] *Institute for Theoretical and Experimental Physics, Moscow, Russia[k]*
[25] *Lebedev Physical Institute, Moscow, Russia[e]*
[26] *Max-Planck-Institut für Physik, München, Germany*
[27] *LAL, Université de Paris-Sud 11, IN2P3-CNRS, Orsay, France*
[28] *LLR, Ecole Polytechnique, IN2P3-CNRS, Palaiseau, France*
[29] *LPNHE, Universités Paris VI and VII, IN2P3-CNRS, Paris, France*
[30] *Faculty of Science, University of Montenegro, Podgorica, Serbia and Montenegro[e]*
[31] *Institute of Physics, Academy of Sciences of the Czech Republic, Praha, Czech Republic[h]*
[32] *Faculty of Mathematics and Physics, Charles University, Praha, Czech Republic[h]*
[33] *Dipartimento di Fisica Università di Roma Tre and INFN Roma 3, Roma, Italy*
[34] *Institute for Nuclear Research and Nuclear Energy, Sofia, Bulgaria[e]*
[35] *Paul Scherrer Institut, Villigen, Switzerland*
[36] *Fachbereich C, Universität Wuppertal, Wuppertal, Germany*
[37] *Yerevan Physics Institute, Yerevan, Armenia*
[38] *DESY, Zeuthen, Germany*
[39] *Institut für Teilchenphysik, ETH, Zürich, Switzerland[i]*
[40] *Physik-Institut der Universität Zürich, Zürich, Switzerland[i]*

[41] *Also at Physics Department, National Technical University, Zografou Campus, GR-15773 Athens, Greece*

[42] *Also at Rechenzentrum, Universität Wuppertal, Wuppertal, Germany*

[43] *Also at University of P.J. Šafárik, Košice, Slovak Republic*

[44] *Also at CERN, Geneva, Switzerland*

[45] *Also at Max-Planck-Institut für Physik, München, Germany*

[46] *Also at Comenius University, Bratislava, Slovak Republic*

[†] *Deceased*

1 Introduction

Recently several fixed-target experiments have published evidence for the production of a strange pentaquark[1] Θ^+ [1], a hypothetical baryon [2] with a minimal quark content of $uudd\bar{s}$, observed in the decay channels K^+n and K_s^0p. This state has been reported with masses in the range of 1520 to 1540 MeV and with a narrow width, consistent with the experimental resolution in most of the observations. Evidence for Θ^+ production has been also obtained in deep inelastic ep scattering (DIS) at HERA by the ZEUS experiment [3]. Many non-observations have also been reported [1]. The experimental situation is thus controversial and further data are needed to establish the existence of this resonance.

This paper presents a search for the strange pentaquark Θ^+ using $74\,\text{pb}^{-1}$ of deep inelastic ep scattering data taken with the H1 detector in the years 1996-2000. A narrow resonance is searched for in the K_s^0p or $K_s^0\bar{p}$ decay channel in the mass range from 1.48 to 1.7 GeV and in the kinematic range of negative four momentum transfer squared, Q^2, from 5 to 100 GeV^2 and of inelasticity, y, from 0.1 to 0.6.

2 Experimental Procedure

2.1 H1 Apparatus

A detailed description of the H1 detector can be found in [4]. The following briefly describes only those detector components important for the present analysis.

The tracks from charged particles used in this analysis are reconstructed in the central tracker, whose main components are two cylindrical drift chambers, the inner and outer central jet chamber (CJCs). The inner and outer CJC are mounted concentrically around the beam-line, covering the range of pseudorapidities[2] $-1.9 < \eta < 1.9$ for tracks coming from the nominal event vertex. The CJCs lie within a homogeneous magnetic field of 1.15 T which allows the transverse momentum, p_T, of charged particles to be measured. Two additional drift chambers complement the CJCs by precisely measuring the z coordinates of track segments and hence assist in the determination of polar angles. Two cylindrical multi-wire proportional chambers facilitate triggering on tracks. The transverse momentum resolution of the central tracker is $\sigma(p_\text{T})/p_\text{T} \simeq 0.005\,p_\text{T}\,/\,\text{GeV} \oplus 0.015$. Charge misidentification is negligible for particles originating from the primary vertex and having transverse momenta in the range relevant to this analysis.

The specific ionisation energy loss of charged particles, dE/dx, is derived from the mean of the inverse square-root of the charge collected by all CJC sense wires with a signal above a certain threshold. The average resolution for minimum ionising particles is $\sigma(dE/dx)/(dE/dx) \simeq 8\%$ [5].

---

[1]In this paper particle names are used to refer to both the particle and its antiparticle, unless explicitly stated otherwise.

[2]The pseudorapidity is given by $\eta = -\ln\tan\theta/2$, where the polar angle θ is measured with respect to the z axis given by the proton beam direction.

A lead/scintillating-fibre calorimeter (SpaCal) is located in the direction of the electron beam and covers the pseudorapidity range $-1.39 < \eta < -3.64$. It contains electromagnetic and hadronic sections and is used here to detect the scattered electron in DIS events and to measure its energy. A planar drift chamber, positioned in front of the SpaCal, measures the polar angle of the scattered electron track originating from the event vertex. The global properties of the hadronic final state are reconstructed combining information from the central tracker, the SpaCal and the Liquid Argon calorimeter, which surrounds the central tracker. The DIS events studied in this paper are triggered on the basis of an energy deposition detected in the SpaCal, complemented by signals in the CJCs and the multi-wire proportional chambers.

The luminosity measurement is based on the Bethe-Heitler process $ep \rightarrow ep\gamma$, where the photon is detected in a calorimeter located downstream of the interaction point.

2.2 Monte Carlo Simulation of Θ^+

To estimate the acceptance for the detection of a hypothetical Θ^+ state, a Monte Carlo simulation based on the RAPGAP 3.1 [6] event generator is used, incorporating the Lund string model fragmentation [7] as implemented in PYTHIA 6.2 [8]. The kinematic distributions of strange baryons in DIS data are reasonably well described [9] by RAPGAP. The Θ^+ is introduced by changing the mass of the Σ^{*+} to values in the range from 1.48 to 1.7 GeV and forcing it to decay to $K_s^0 p$. By doing so, it is assumed that the Θ^+ is produced at pseudorapidities and transverse momenta similar to those of other strange baryons and that it decays isotropically. In this simulation the Θ^+ particle is produced on mass shell. The generated events are passed through the H1 detector simulation based on GEANT [10] and are then subjected to the same reconstruction and analysis chain as are the data.

2.3 Selection of DIS Events

The analysis is carried out using data corresponding to an integrated luminosity of $\mathscr{L} = 74 \, \text{pb}^{-1}$, taken in the years 1996-2000. During this time HERA collided electrons[3] at an energy of 27.6 GeV with protons at 820 GeV (1996-1997) and 920 GeV (1998-2000)[4].

Events are selected if the z coordinate of the event vertex, reconstructed using the central tracker, lies within 35 cm of the mean position for ep interactions. The scattered electron is required to be reconstructed in the SpaCal with an energy, E_e, above 11 GeV. The negative four momentum transfer squared of the exchanged virtual photon, Q^2, is required to lie in the range $5 < Q^2 < 100 \, \text{GeV}^2$, as reconstructed from the energy and polar angle of the scattered electron. The inelasticity y of the event is reconstructed using the scattered electron kinematics and is required to be in the range $0.1 < y < 0.6$. The lower cut on y ensures that the hadronic final state lies in the central region of the detector, whilst the upper cut corresponds approximately to the cut on E_e. The difference between the total energy E and the longitudinal component of

---

[3]The analysis uses data from periods when the beam lepton was either a positron ($\mathscr{L} = 65 \, \text{pb}^{-1}$) or an electron ($\mathscr{L} = 9 \, \text{pb}^{-1}$).

[4]The sample with a proton energy of 820 (920) GeV corresponds to a luminosity of $\mathscr{L} = 18 \, (56) \, \text{pb}^{-1}$, resulting in an effective $\sqrt{s} = 314$ GeV for the total sample.

the total momentum p_z, calculated from the electron and the hadronic final state, is restricted to $35 < E - p_z < 70$ GeV. This requirement suppresses photoproduction background, in which the electron escapes detection and a hadron fakes the electron signature.

2.4   Selection of K_s^0 Meson and Proton Candidates

The analysis is based on charged particles reconstructed in the central tracker. Tracks are accepted if they have transverse momenta $p_T > 0.15$ GeV and pseudorapidities $|\eta| < 1.75$. The K_s^0 meson is identified through its decay into charged pions, $K_s^0 \to \pi^+\pi^-$. Events are accepted if they contain at least one K_s^0 candidate and at least one proton candidate track originating from the primary vertex.

K_s^0 candidates are searched for by performing a constrained fit to each pair of oppositely charged tracks. The fit demands these tracks to originate at a common secondary decay vertex and the decaying neutral particle to come from the primary vertex. The secondary vertex must be radially displaced by at least 2 cm from the primary interaction point. The candidates are required to have a transverse momentum $p_T(K_s^0) \geq 0.3$ GeV and a pseudorapidity $|\eta(K_s^0)| \leq 1.5$. Contamination from Λ production is eliminated by requiring that the invariant mass $M_{p\pi}$ of the two tracks, reconstructed assigning the proton (pion) mass to the track with higher (lower) momentum, be above 1.125 GeV. Background from converted photons is rejected by the requirement $M_{ee} > 50$ MeV. Figure 1a shows the distribution of the invariant mass $M_{\pi^+\pi^-}$ of the K_s^0 candidates together with a fit to the data using a superposition of two Gaussian functions (to account for different invariant mass resolutions in different decay topologies) and a straight line to approximate the background. The fitted peak position is $M_{\pi^+\pi^-} = 495.9$ MeV which agrees with the nominal K_s^0 mass [11] within a few per mill. 133,000 K_s^0 candidates are reconstructed, as given by subtracting the fitted background from the data. K_s^0 candidates with $0.475 < M_{\pi^+\pi^-} < 0.515$ GeV are selected for further analysis. In this mass range the background under the K_s^0 peak is $\sim 3\%$.

Proton candidates are selected using requirements on the specific ionisation energy loss, dE/dx, measured in the CJCs. Figure 1b shows the measured dE/dx plotted against momentum for all tracks originating from the primary vertex, which lead to a mass $M_{K_s^0 p} < 1.8$ GeV when combined with the K_s^0 candidates. The curves in Fig. 1b represent the most probable dE/dx values as derived from a phenomenological parameterisation [5] based on the Bethe-Bloch formula. Likelihoods for a particle to be a pion, kaon or proton are obtained from the difference between the measured dE/dx and the most probable value for each particle type at the reconstructed momentum. The normalised proton likelihood, L_p, is defined as the ratio of the proton likelihood to the sum of the pion, kaon and proton likelihoods. In order to optimise simultaneously the background suppression and the proton selection efficiency, a momentum dependent cut on the normalised proton likelihood L_p is applied of $L_p > 0.3$ ($L_p > 0.1$) for proton momenta below (above) 2 GeV. The efficiency of the dE/dx selection is tested using protons from Λ decays. The efficiency varies between 65% and 100% as a function of momentum and is described by the Monte Carlo simulation to within 5%.
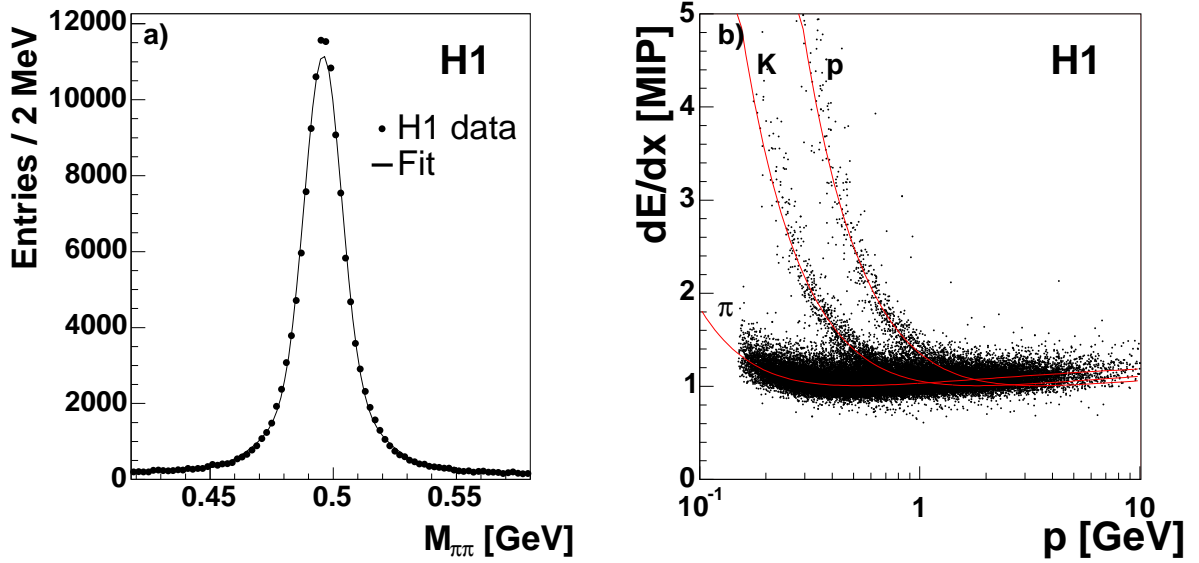
Figure 1: a) Inclusive K_s^0 signal in the invariant $\pi^+\pi^-$ mass distribution for $5 < Q^2 < 100 \, \text{GeV}^2$ together with the result from a fit of a sum of two Gaussian functions for the signal and a straight line for the background. b) Specific ionisation energy loss relative to that of a minimally ionising particle plotted as a function of momentum. The lines indicate parameterisations of the most probable energy loss for pions, kaons and protons measured in the CJCs.

3 Analysis of $K_s^0 p$ Combinations

In order to search for a Θ^+ resonance, the candidate K_s^0 mesons are combined with the proton candidates. To improve the mass resolution the $K_s^0 p$ four vector is calculated as the sum of the K_s^0 and proton four vectors with $E_{K_s^0} = \sqrt{p_{K_s^0}^2 + M_{K_s^0}^2}$, where the nominal mass $M_{K_s^0}$ is used instead of $M_{\pi^+\pi^-}$. For the $K_s^0 p$ system, $p_{\mathrm{T}}(K_s^0 p) > 0.5 \, \text{GeV}$ and $|\eta(K_s^0 p)| < 1.5$ are required. The $M_{K_s^0 p}$ distributions are shown in Fig. 2 for three bins in Q^2 ($5 < Q^2 < 10 \, \text{GeV}^2$, $10 < Q^2 < 20 \, \text{GeV}^2$ and $20 < Q^2 < 100 \, \text{GeV}^2$). The shape of the invariant mass distributions is found to be reproduced by a background Monte Carlo simulation of inclusive DIS events using the DJANGOH event generator [12] and the H1 detector simulation based on GEANT. A fit of an empirical background function of the form

$$f(M_{K_s^0 p}) = \alpha \cdot (M_{K_s^0 p} - M_{thr})^\beta \cdot \exp\{-(M_{K_s^0 p} - M_{thr}) \cdot \gamma\} \tag{1}$$

is performed to the data, where $M_{thr} = M_{K_s^0} + M_p$ (M_p being the proton mass) and α, β and γ are free parameters determined for each Q^2 interval independently. The data are well described by this phenomenological function. No narrow resonance is observed in any of the Q^2 bins. The $M_{K_s^0 p}$ distribution is therefore used to set upper limits on the Θ^+ production cross section,

$$\sigma^\Theta \equiv (\sigma(ep \to e\Theta^+ X) + \sigma(ep \to e\overline{\Theta^+} X)) \times BR(\Theta^+ \to K^0 p) \quad .$$

Since the mass of the Θ^+ candidate is experimentally not well established, mass dependent limits are derived in the range from 1.48 to 1.7 GeV. For a given Θ^+ mass, M_{Θ^+}, the expected
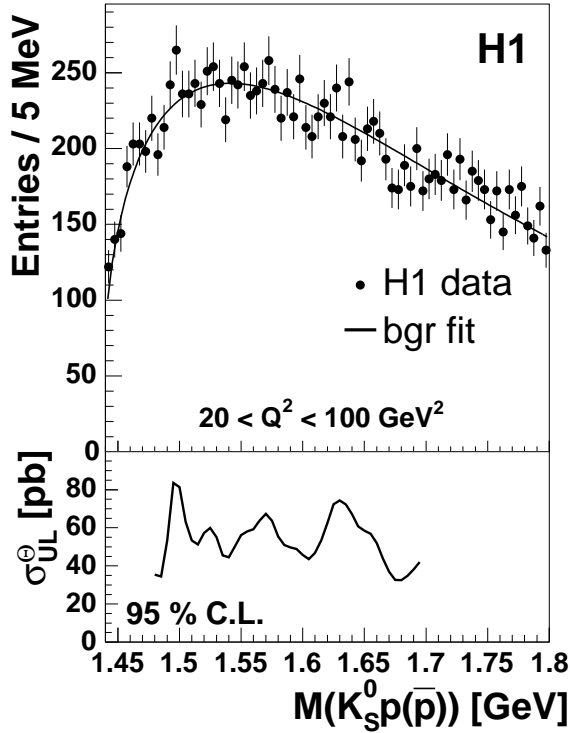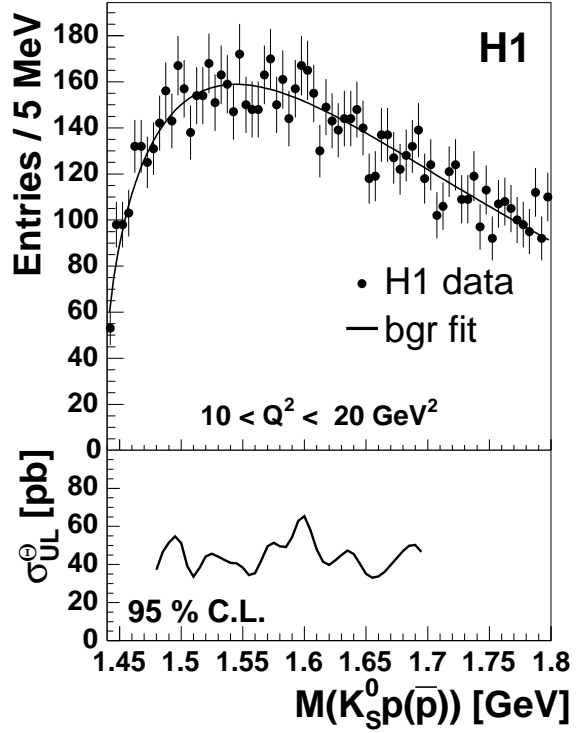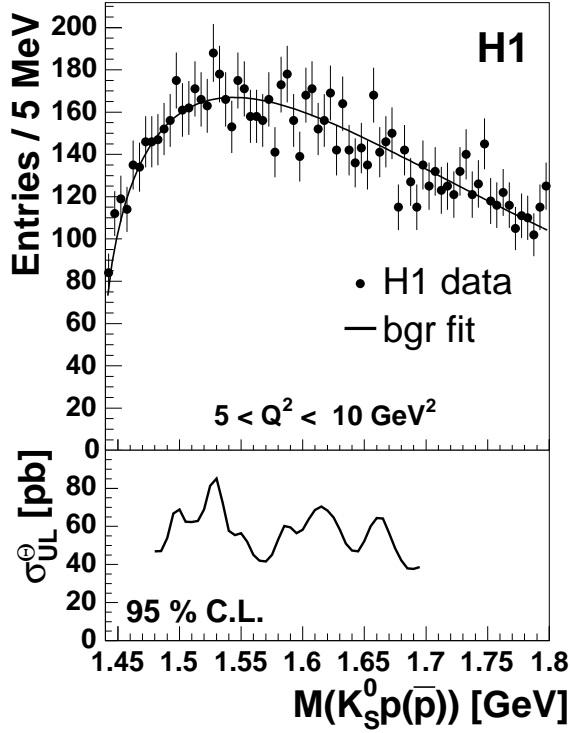
Figure 2: Invariant $K^0_s p(\bar{p})$ mass spectra in bins of Q^2. The full line shows the result from the fit of the background function (1) to the data. The upper limits on the cross section σ^{Θ}_{UL} (see text) at 95% confidence level integrated over the kinematic range $p_T(K^0_s p) > 0.5\,\mathrm{GeV}$, $|\eta(K^0_s p)| < 1.5$ and $0.1 < y < 0.6$ are shown below the mass spectra.

8

number of selected $K_s^0 p$ combinations due to Θ^+ production is related to σ^Θ via

$$N(M_{\Theta^+}) = \sigma^\Theta \cdot \mathscr{L} \cdot \varepsilon_{DIS} \cdot \varepsilon_{\Theta^+}(M_{\Theta^+}) \cdot BR(K^0 \to \pi^+\pi^-) \quad , \tag{2}$$

where $\mathscr{L}$ is the integrated luminosity, ε_{DIS} is the acceptance of the inclusive DIS event selection and $\varepsilon_{\Theta^+}(M_{\Theta^+})$ is the acceptance of the Θ^+ selection. The cross section σ^Θ is integrated over the visible kinematic range studied, which is given by $p_T(K_s^0 p) > 0.5\,\text{GeV}$, $|\eta(K_s^0 p)| < 1.5$, $0.1 < y < 0.6$ and the respective Q^2 bin. The branching ratio for the transition of K^0 to K_s^0 and its decay into charged pions is $BR(K^0 \to \pi^+\pi^-) = BR(K^0 \to K_s^0) \times BR(K_s^0 \to \pi^+\pi^-) = 0.5 \times (0.6895 \pm 0.0014)$ [11].

An upper limit at the 95% confidence level (C.L.) on $N(M_{\Theta^+})$, $N_{UL}(M_{\Theta^+})$, is obtained from the observed, the background and the signal $M_{K_s^0 p}$ distributions in the mass range from 1.45 to 1.8 GeV, using a modified frequentist approach based on likelihood ratios [13]. This takes into account statistical and systematic uncertainties of the signal and the background number of $K_s^0 p$ combinations. The $M_{K_s^0 p}$ distribution for signal combinations is taken to be a Gaussian with a mean M_{Θ^+} and a width corresponding to the experimental mass resolution as obtained in the Θ^+ Monte Carlo simulations. This width $\sigma(M_{\Theta^+})$ varies from 4.8 to 11.3 MeV in the mass range from 1.48 to 1.7 GeV. The background $M_{K_s^0 p}$ distribution is taken to be the fitted function given by equation (1).

A systematic uncertainty on this background distribution is assessed by performing the fit under different assumptions: using the background function (1) in the full mass range, excluding a mass window of $\pm 2\sigma$ around the Θ^+ mass, and also using the sum of the background function and a Gaussian with fixed mass M_{Θ^+} and width $\sigma(M_{\Theta^+})$ to account for a possible signal. The uncertainty of the number of background $K_s^0 p$ combinations is estimated from the difference between the different fitting methods and amounts to 2%.

The systematic uncertainty of $N(M_{\Theta^+})$ comprises the following main contributions:

- The measurement of the luminosity has an uncertainty of 1.5%.

- The uncertainty of the inclusive DIS event selection, ε_{DIS}, is 6.5%, which is coming mainly from contributions due to the trigger efficiency (5%), the SpaCal energy calibration (3%), remaining contamination from photoproduction background (2.5%) and radiative corrections (1%).

- The efficiency of the Θ^+ selection, $\varepsilon_{\Theta^+}(M_{\Theta^+})$, has an uncertainty of 8% which comprises the uncertainty in modelling track losses (6%) and the uncertainty in the efficiency of the dE/dx selection (5%).

- The Monte Carlo model used for correction is based on the assumption that pentaquarks are produced with similar phase space distributions as strange baryons. Since no established production mechanism for the Θ^+ yet is known, production model dependent uncertainties are not considered. Dependencies on the QCD models are estimated by comparing the Θ^+ acceptances derived with the RAPGAP and the CASCADE [14] event generators, which incorporate different QCD evolution schemes. The difference is found to be small and negligible compared with other sources of systematic uncertainties.

9

The contributions are added in quadrature and the resulting total systematic uncertainty of $N(M_{\Theta^+})$ is 11%. The uncertainty of the number of background $K_s^0 p$ combinations is the dominating systematic effect in the limit calculation.

The upper limit on the cross section, σ_{UL}^Θ, is then calculated from $N_{UL}(M_{\Theta^+})$ according to equation (2). The upper limits at 95% C.L. are shown below the mass spectra of Fig. 2 for the three different Q^2 bins. The limits vary between 30 and 90 pb for the different Q^2 bins and over the mass range from 1.48 to 1.7 GeV. The invariant mass spectra of positive $K_s^0 p$ and negative $K_s^0 \bar{p}$ combinations are also studied separately. No narrow resonance is observed. The corresponding upper limits for the Θ^+ decaying to $K^0 p$ and its charge conjugate $\overline{\Theta^+}$ decaying to $\overline{K^0}\bar{p}$, shown in Fig. 3, are found to be of comparable size. The up- and downward fluctuations of the limits occur at different masses for the different Q^2 bins and charges, which supports the hypothesis that the observed $K_s^0 p$ invariant mass distributions are consistent with being due to combinatorial background only.

The ZEUS experiment has reported a positive Θ^+ observation at a mass of 1.522 GeV in DIS for $Q^2 \geq 20$ GeV^2 using a data sample corresponding to an integrated luminosity of 121 pb^{-1} [3]. The $K_s^0 p$ system was reconstructed using only protons having a momentum below 1.5 GeV, while the requirements on the transverse momenta and pseudorapidities of K_s^0 and $K_s^0 p$ are the same as in the present analysis. The analysis described above is repeated using only proton candidates with momenta below 1.5 GeV. The resulting invariant $K_s^0 p(\bar{p})$ mass spectra are shown in Fig. 4a for $20 < Q^2 < 100$ GeV^2 and $0.1 < y < 0.6$. No significant pentaquark signal is observed for events in the low momentum proton selection. The upper limits σ_{UL}^Θ at 95% C.L., derived from these mass spectra, are shown in Fig. 4b. At a Θ^+ mass of 1.52 GeV an upper limit on the cross section of 72 pb at 95% C.L. is found. The $K_s^0 p$ and $K_s^0 \bar{p}$ combinations do not yield any significant peak either. The corresponding upper limits are also shown in Fig. 4c.

4   Conclusions

A search for the strange pentaquark Θ^+ in deep inelastic ep scattering is presented. No signal for Θ^+ production is observed in the decay mode $\Theta^+ \to K_s^0 p$ and $\overline{\Theta^+} \to K_s^0 \bar{p}$ for negative momentum transfers squared, Q^2, between 5 and 100 GeV^2. Assuming that pentaquarks are produced with similar kinematics as known strange baryons, mass dependent upper limits at 95% confidence level on the cross section $\sigma(ep \to e\Theta^+ X) \times BR(\Theta^+ \to K^0 p)$ are derived in intervals of Q^2 and found to vary between 30 and 90 pb over the mass range from 1.48 to 1.7 GeV.

The analysis is repeated, restricted to large Q^2 and low proton momentum, a region in which the ZEUS collaboration observes evidence for a Θ^+ signal. For this selection no signal is found either.
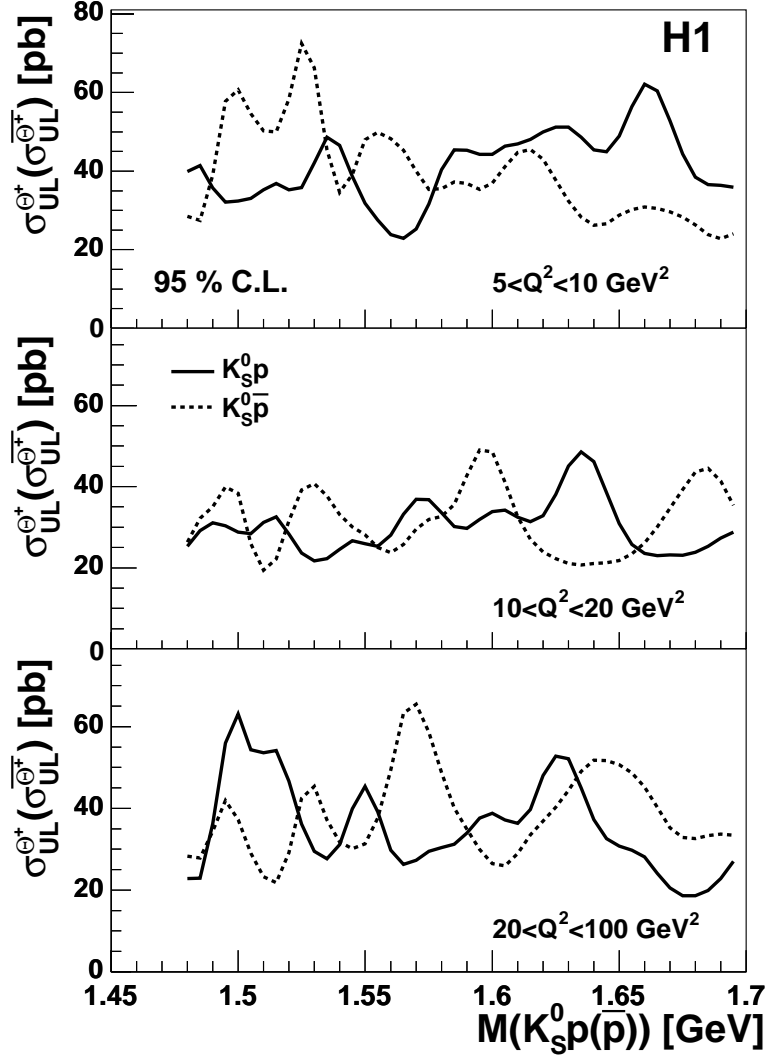
Figure 3: Upper limits on the cross section σ^{Θ}_{UL} (see text) at 95% confidence level in bins of Q^2 for $K^0_s p$ (full line) and $K^0_s \bar{p}$ (dashed line) separately, integrated over the kinematic range $p_{\mathrm{T}}(K^0_s p) > 0.5$ GeV, $|\eta(K^0_s p)| < 1.5$ and $0.1 < y < 0.6$.
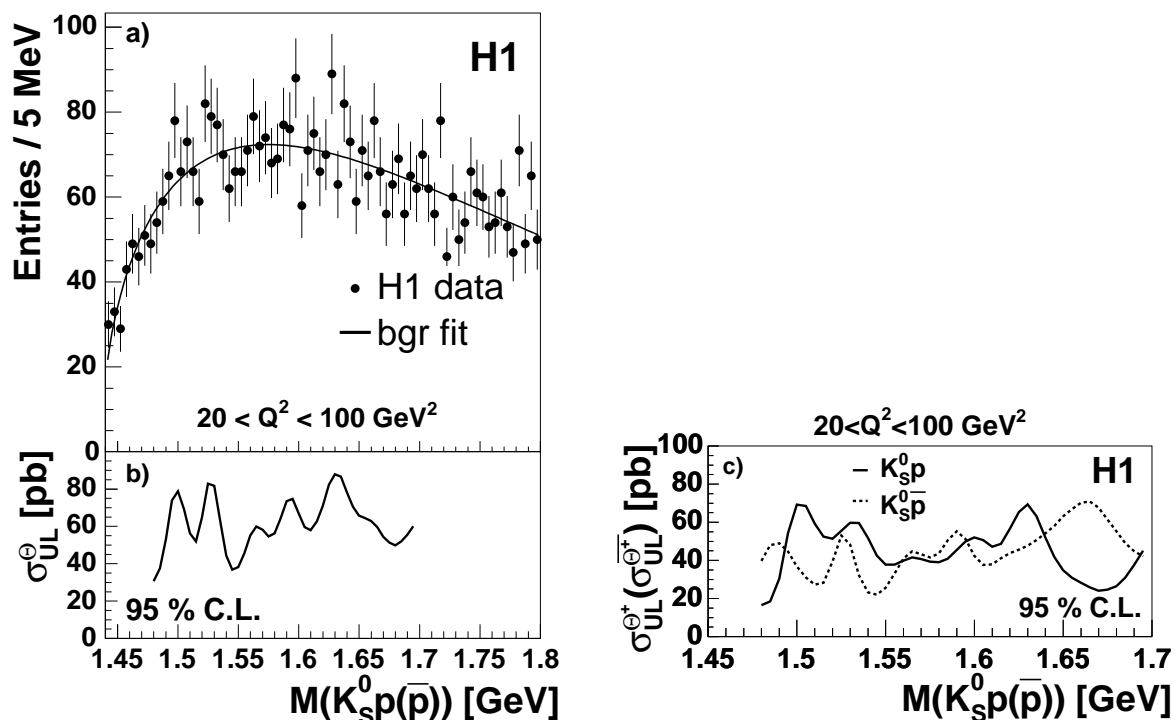
Figure 4: a) Invariant $K_s^0 p(\bar{p})$ mass spectra for $20 < Q^2 < 100\,\mathrm{GeV}^2$ for proton candidates with momenta below $1.5\,\mathrm{GeV}$ and b) upper limits on the cross section σ_{UL}^{Θ} (see text) at 95% confidence level for $20 < Q^2 < 100\,\mathrm{GeV}^2$ integrated over the kinematic range $p_{\mathrm{T}}(K_s^0 p) > 0.5\,\mathrm{GeV}$, $|\eta(K_s^0 p)| < 1.5$ and $0.1 < y < 0.6$ using the low momentum proton selection for all $K_s^0 p$ combinations and c) for $K_s^0 p$ (full line) and $K_s^0 \bar{p}$ (dashed line) combinations separately.

Acknowledgements

References

[1] K. Hicks, Prog Part. Nucl. Phys. **55** (2005) 647 [hep-ex/0504027].

[2] D. Diakonov, V. Petrov and M. Polyakov, Z. Phys. A **359**, 305 (1997) [hep-ph/9703373];
R. L. Jaffe and F. Wilczek, Phys. Rev. Lett. **91** (2003) 23 [hep-ph/0307341];
M. Karliner and H. Lipkin, Phys. Lett. **B575** (2003) 249 [hep-ph/0307243];
for a review on pentaquark phenomenology see R. L. Jaffe, Phys. Rept. **409** (2005) 1 [hep-ph/0409065].

12

[3] S. Chekanov *et al.* [ZEUS Collaboration], Phys. Lett. **B591** (2004) 7 [hep-ex/0403051].

[4] I. Abt *et al.* [H1 Collaboration], Nucl. Inst. Meth. A **386** (1997) 310;
    I. Abt *et al.* [H1 Collaboration], Nucl. Inst. Meth. A **386** (1997) 348;
    R. D. Appuhn *et al.* [H1 SpaCal Group], Nucl. Inst. Meth. A **386** (1997) 397;
    C. Adloff *et al.* [H1 Collaboration], Eur. Phys. J. C **21** (2001) 33.

[5] J. Steinhart, Ph.D. thesis, 1999, Universität Hamburg (in German), available from
    http://www-h1.desy.de/publications/theses_list.html.

[6] H. Jung, Comput. Phys. Commun. **71** (1992) 15.

[7] B. Andersson, G. Gustafson, G. Ingelman and T. Sjöstrand, Phys. Rept. **97** (1983) 31.

[8] T. Sjöstrand *et al.*, Comput. Phys. Commun. **135** (2001) 238 [hep-ph/0010017].

[9] M. Derrick *et al.* [ZEUS Collaboration], Z. Phys. C **68** (1995) 29 [hep-ex/9505011];
    S. Aid *et al.* [H1 Collaboration], Nucl. Phys. B **480** (1996) 3 [hep-ex/9607010];
    C. Risler, Ph.D. thesis, 2004, Universität Hamburg (in German), available from
    http://www-h1.desy.de/publications/theses_list.html.

[10] R. Brun *et al.*, GEANT3, Technical Report CERN-DD/EE/84-1, CERN, 1987.

[11] Particle Data Group, S. Eidelman *et al.*, Phys. Lett. **B592** (2004) 1.

[12] K. Charchula, G.A. Schuler and H. Spiesberger, Comput. Phys. Commun. **81** (1994) 381.

[13] T. Junk, Nucl. Inst. Meth. A **434** (1999) 435 [hep-ex/9902006].

[14] H. Jung and G.P. Salam, Eur. Phys. J. C **19** (2001) 351 [hep-ph/0012143];
    H. Jung, Comput. Phys. Commun. **143** (2002) 100 [hep-ph/0109102].